

Structure–Activity Relationship of a Series of Inhibitors of Monoacylglycerol Hydrolysis—Comparison with Effects upon Fatty Acid Amide Hydrolase[†]

José Antonio Cisneros,^{‡,§} Séverine Vandevorde,^{‡,||,⊥} Silvia Ortega-Gutiérrez,[§] Clément Paris,[§] Christopher J. Fowler,[⊥] and María L. López-Rodríguez^{*,§}

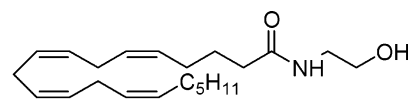
Departamento de Química Orgánica I, Facultad de Ciencias Químicas, Universidad Complutense, E-28040 Madrid, Spain, and Department of Pharmacology and Clinical Neuroscience, Umeå University, Umeå, Sweden

Received June 5, 2007

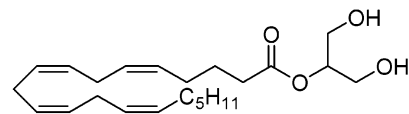
A series of 32 heterocyclic analogues based on the structure of 2-arachidonoylglycerol (2-AG) were synthesized and tested for their ability to inhibit monoacylglycerol lipase and fatty acid amide hydrolase activities. The designed compounds feature a hydrophobic moiety and different heterocyclic subunits that mimic the glycerol fragment. This series has allowed us to carry out the first systematic structure–activity relationship study on inhibition of 2-AG hydrolysis. The most promising compounds were oxiran-2-ylmethyl (5*Z*,8*Z*,11*Z*,14*Z*)-icosa-5,8,11,14-tetraenoate (**1**) and tetrahydro-2*H*-pyran-2-ylmethyl (5*Z*,8*Z*,11*Z*,14*Z*)-icosa-5,8,11,14-tetraenoate (**5**). They inhibited cytosolic 2-oleoylglycerol (2-OG) hydrolysis completely (IC₅₀ values of 4.5 and 5.6 μM, respectively). They also blocked, albeit less potently, 2-OG hydrolysis in membrane fractions (IC₅₀ values of 19 and 26 μM, respectively) and anandamide hydrolysis (IC₅₀ values of 12 and 51 μM, respectively). These compounds will be useful in delineating the importance of the cytosolic hydrolytic activity in the regulation of 2-AG levels and, hence, its potential as a target for drug development.

Introduction

Endocannabinoids constitute a class of lipid messengers that modulate a broad number of physiological processes both in the central nervous system and in the periphery.¹ *N*-arachidonylethanolamine (anandamide, AEA^o) and 2-arachidonoylglycerol (2-AG) are at present considered to be the main endogenous ligands for the CB₁ and CB₂ cannabinoid receptors (Figure 1). During the past decade these endogenous ligands and their receptors have been characterized (see ref 2 for a review of the pharmacology of the endocannabinoids and their receptors), and their involvement in a broad range of physiological functions including regulation of several neurotransmitter systems,³ memory control,⁴ analgesia,⁵ or appetite⁶ has been described. More interesting from a medicinal chemistry point of view is their influence in several pathologies, a fact that supports the suitability of the endogenous CB system (ECS) as a therapeutic target for the treatment of disorders such as neurodegenerative diseases, pain, cancer, and obesity.^{1,7–11} Until recently, AEA has constituted the major focus of research, but nowadays increasing evidence points out the prominent, and sometimes underestimated, role of 2-AG in the regulation of different functions, not the least being retrograde signaling in the brain.^{12–14}



Anandamide



2-Arachidonoylglycerol

Figure 1. Structure of the endocannabinoids *N*-arachidonylethanolamine (anandamide, AEA) and 2-arachidonoylglycerol (2-AG).

The involvement of endocannabinoids in the regulation of such a broad number of pathologies opens the possibility of conceiving novel therapeutic approaches based on the pharmacological regulation of their levels. Physiologically, regulation of the levels of endocannabinoids relies on the enzymes responsible for their synthesis and degradation. With respect to the latter, the most important pathways are hydrolytic. In the case of AEA, the enzyme in question is fatty acid amide hydrolase (FAAH)¹⁵ and its role in the regulation of the levels of this endocannabinoid has been unequivocally demonstrated.¹⁶ FAAH inhibitors such as URB597¹⁷ (Figure 2) are currently of considerable interest, given that they produce potentially useful effects in models of inflammation and pain without producing the psychotropic effects seen with direct acting CB₁ receptor agonists.^{17–19} Although FAAH can also metabolize 2-AG in vitro,²⁰ and some FAAH inhibitors such as URB597 or *N*-arachidonoylserotonin can induce increases in 2-AG levels in certain models,^{21–23} genetic elimination or chemical inhibition of this enzyme has been reported not to affect brain 2-AG levels in vivo.^{17,24} However, these two findings can be conciliated taking into account the possibility of the development of redundant pathways or compensatory mechanisms caused by

[†] Dedicated to Prof. Miguel Yus on the occasion of his 60th birthday.

* To whom correspondence should be addressed. Phone: 34-91-3944239. Fax: 34-91-3944103. E-mail: mluzlr@quim.ucm.es.

[‡] These authors contributed equally to the work.

[§] Universidad Complutense.

^{||} Present address: Unité de Chimie Pharmaceutique et de Radiopharmacie, Université Catholique de Louvain, Avenue Mounier 73, UCL-CMFA 73.40, B-1200 Brussels, Belgium.

[⊥] Umeå University.

^o Abbreviations: AEA, anandamide; AEA-m, anandamide hydrolysis in membrane fractions; 2-AG, 2-arachidonoylglycerol; CB, cannabinoid; DAGL *sn*-1 selective diacylglycerol lipase; ECS, endocannabinoid system; FAAH, fatty acid amide hydrolase; MGL monoacylglycerol lipase; 2-OG, 2-oleoylglycerol; 2-OG-c 2-oleoylglycerol hydrolysis in cytosolic fractions; 2-OG-m, 2-oleoylglycerol hydrolysis in membrane fractions; SAR structure–activity relationship.

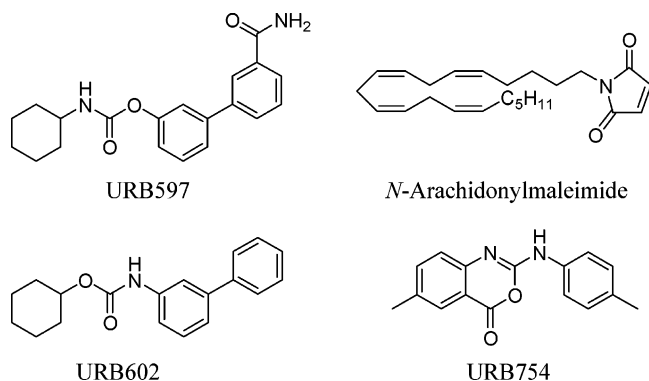


Figure 2. Structure of the endocannabinoid degradation inhibitors URB597, *N*-arachidonylmaleimide, URB602 and URB754.

chronic absence of FAAH in knockout mice or the existence of alternative catabolic pathway for 2-AG such as its acyl rearrangement to 1-AG or its direct incorporation into phospholipids.²⁵ Regardless of these possibilities, it is clear that FAAH is not the only enzyme responsible for the *in vivo* inactivation of 2-AG, and monoacylglycerol lipase (MGL) has been suggested to play a more important role in this respect.²⁶ This enzyme is a 33 kDa soluble serine hydrolase that cleaves 1(3)- and 2-monoacylglycerols and features the structural motifs typical of other lipases including the HG dipeptide motif and the α/β hydrolase fold.^{26–28} MGL is abundantly expressed in areas of the brain where CB₁ receptors are also found and it shows preference for 2-AG versus AEA *in vitro*.²⁶

Given the role of 2-AG in the regulation of (patho)-physiological events, an obvious strategy to pursue would be the development of compounds that inhibit its hydrolysis, in analogy with the situation for FAAH. Two issues, however, need to be considered. First, whereas FAAH has been validated as a drug target based on *in vivo* data derived from knockout and transgenic models,^{16,24,29} its three-dimensional (3D) structure has been solved,³⁰ structure–activity relationship (SAR) studies have been described, and potent and selective inhibitors characterized,^{31–33} however, all these aspects are lacking for MGL. For instance, very little is known about the structure of MGL or which residues are located in the vicinity of the active site and therefore could be used for the design of new inhibitors. In this regard, and based on the initial data about MGL sensitivity to free sulfhydryl group-modifying agents, Saario and co-workers³⁴ developed a series of maleimide derivatives, identifying *N*-arachidonylmaleimide (Figure 2, IC₅₀ = 140 nM) as the most potent inhibitor of 2-AG hydrolysis of their series. However, nothing has been mentioned about its selectivity for other enzymes of the ECS, such as the *sn*-1 selective diacylglycerol lipases α and β (DAGL α and DAGL β), which are also sensitive to nonspecific cysteine hydrolase inhibitors³⁵ or, in general, for other cysteine-containing proteins.

A second issue concerns the contribution made by MGL to the total 2-AG hydrolytic capacity of the tissue in question. Although MGL overexpression increases and immunodepletion decreases, respectively, the hydrolytic capacity of the samples toward 2-AG and its alternative substrate 2-oleoylglycerol (2-OG),^{26,36} this does not rule out a contribution by additional 2-AG/2-OG hydrolyzing enzymes. Indeed, in the pig brain, for example, at least two chromatographically distinct 2-AG-hydrolyzing activities have been reported.³⁷ A novel 2-AG hydrolytic activity has also been identified and characterized in microglial cells.³⁸ These observations mean that the approach that should be taken is dependent upon the scientific question to be answered. Thus, development of new compounds that are

specifically MGL inhibitors, that is, screened against the recombinant enzyme, may shed light on the contribution of this enzyme to the total hydrolysis of 2-AG. So far, there is only limited information published in this respect, although the rat brain cytosolic activity is inhibited by some compounds with potencies similar to those seen with recombinant MGL when data from the same laboratories are compared.^{12,39,40}

The alternative approach is to use tissue extracts to identify compounds that produce a total inhibition of enzymatic hydrolysis of 2-AG (or 2-OG) without affecting AEA activity. This latter approach has immediate importance in order to dissect the actions of this endocannabinoid from those of AEA. At this stage, most published pharmacological studies with respect to 2-AG/2-OG inhibition have taken this latter route using either cytosolic or membrane fractions from brain.^{41–44} Given that the present study also follows this route, we have referred throughout to effects upon 2-OG (or 2-AG when appropriate) hydrolysis rather than upon MGL. In general, compounds inhibiting brain 2-OG/2-AG hydrolysis are few and far between and can be classified into two main groups. The first class comprises closely related 2-AG analogues in which the arachidonic acid moiety has been replaced by other fatty acid chains with different degrees of saturation,^{41,42} along with several cyclooxygenated analogues of 1-arachidonoylglycerol.⁴³ However, all of them showed moderate potency to inhibit 2-OG hydrolysis (IC₅₀ values ranging from 5 to 84 μ M) as well as weak selectivity upon FAAH,^{41–43} but they may be useful as templates for further synthesis. A second strategy aimed at the identification of MGL inhibitors with completely different structural cores has also been undertaken. Hence, based on the hypothesis that FAAH and MGL should share some structural similarities in their binding pockets, the FAAH inhibitor-inspired *N*-biphenyl carbamate URB602 (Figure 2) was identified.³⁹ This compound inhibits the hydrolysis of 2-OG (IC₅₀ = 28 μ M) by a noncompetitive mechanism.³⁹ The selectivity of this compound in cell-free systems, however, has been questioned.⁴⁵ A second compound, URB754 (Figure 2), was initially proposed as a potent MGL-selective inhibitor,¹² but it has subsequently been shown by these authors that the effects were due to a mercuric contaminant⁴⁶ (see also refs 45 and 47). There is, thus, an acute need to find compounds that can selectively inhibit the hydrolysis of 2-AG. Here, we report the design and synthesis of a new series of compounds of general structure I (Figure 3) and their evaluation as inhibitors of 2-AG hydrolysis (assessed by use of the alternative substrate 2-OG) by rat brain cytosolic and membrane fractions. These data have allowed us to carry out the first systematic SAR study for these hydrolytic activities and to obtain deeper insights in the structural requirements for selectivity vis à vis FAAH.

Chemistry

The synthesis of the esters and amides of general structure I (1–32) listed in Tables 1–5 is indicated in Scheme 1. These compounds were prepared by condensation between the acid and the corresponding amine or alcohol in the presence of dicyclohexylcarbodiimide (DCC) and catalytic amounts of *N,N*-dimethyl-4-aminopyridine (DMAP).

Pharmacological Assays

All synthesized compounds were tested for their ability to inhibit 2-OG and AEA hydrolytic activities using a substrate concentration of 2 μ M and the assay procedures described previously.⁴² [³H]-2-oleoylglycerol ([³H]-2-OG) hydrolysis was measured in membrane and cytosolic fractions prepared from

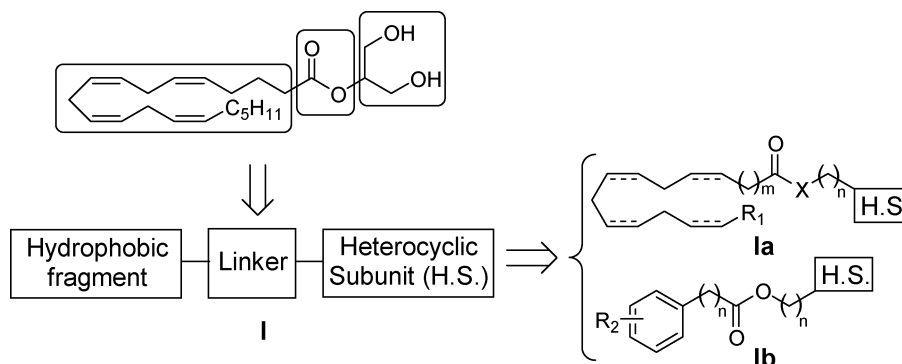
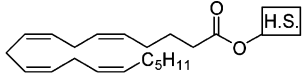


Figure 3. Design of compounds **I(a,b)**.

Table 1. Influence of the Heterocyclic Subunit (H.S.)^a



Cpd	H. S.	pI ₅₀ [IC ₅₀ , μM]		
		2-OG-c	2-OG-m	AEA-m
1		5.35±0.05 [4.5]	4.72±0.05 [19]	4.91±0.05 [12]
2		4.67±0.04 [21]	4.1±0.1 [75]	4.48±0.06 [33]
3		4.37±0.06 [43]	<4 (46±0.5%) ^c	4.98±0.08 [11, 78%] ^b
4		4.3±0.1 [45]	4.0±0.1 [95]	4.0±0.1 [98]
5		5.26±0.04 [5.6]	4.58±0.05 [26]	4.30±0.06 [51]
6		4.5±0.1 [30, 62%] ^b	<4 (33±2%) ^c	5.3±0.2 [5.3, 63%] ^b
7		4.57±0.07 [27]	4.0±0.1 [99]	4.68±0.05 [21]
8		4.35±0.07 [45]	<4 (3±3%) ^c	4.0±0.2 [91]

^a Throughout the tables, the pI₅₀ values (−log[IC₅₀]) are expressed as mean ± sem. The IC₅₀ values derived from the mean pI₅₀ values are given in brackets. ^b When the data was better fitted to an inhibition curve with a residual activity (i.e., the “bottom” value) > 0, the inhibitable component (100 − “bottom” value) is given in the table as maximum inhibition and the data are expressed as [IC₅₀, percentage of maximum inhibition]. ^c When the inhibitable component was less than 50%, when the data could not be fitted to a curve due to a marginal degree of inhibition, or when the pI₅₀ value was lower (and, hence, the IC₅₀ value was higher) than the highest concentration tested (100 μM), the pI₅₀ values have been indicated as <4 (i.e., IC₅₀ value > 100 μM), and the percentage of inhibition attained at 100 μM has been indicated between parentheses as mean ± sem.

rat cerebella. For membrane [³H]-2-OG hydrolysis, the assays were undertaken in the presence of 3 μM URB597 to ensure complete inhibition of FAAH.⁴² [³H]-AEA hydrolysis was determined in rat cerebellum membranes. Data were expressed as % of controls, and the pI₅₀ values (and, hence, IC₅₀ values) were determined as described previously.⁴⁸

Results

In the absence of any potent inhibitor of 2-OG hydrolysis that could be used as lead compound and without an experimentally determined 3D structure of MGL, we took as the

starting point the structure of its endogenous substrate, 2-AG. Accordingly, we designed a series of esters wherein the glycerol moiety was substituted by different heterocyclic subunits, with the objective of introducing structural variations that mimic the glycerol fragment. Additionally, we have studied the effect of modifications in the fatty acid chain as well as in the ester group (Figure 3). We have synthesized a total of 32 compounds and assessed them for their abilities to inhibit the hydrolysis of [³H]-2-OG in cytosolic (2-OG-c) and membrane (2-OG-m) fractions. Effects upon the FAAH-catalyzed hydrolysis of AEA by the membrane fractions were determined in view of the stated aim of the study—to identify compounds that can selectively block monoacylglycerol hydrolysis by the brain without concomitant effects upon AEA hydrolysis. For consistency of notation, FAAH activity is shown in the tables and figures as “AEA-m”. Examples of the concentration–response curves are shown in Figure 4 for compounds **1**, **5**, **16**, and **31**. For the curves of the types seen for **1** and **5**, analysis is very straightforward, and in Tables 1–5, values are presented as pI₅₀ (the negative logarithm of the IC₅₀ value) and the corresponding IC₅₀ values derived from the pI₅₀ values. However, in some cases, 100% inhibition was not seen at the highest dose tested (see, e.g., the inhibition of 2-OG-m by **16** or of 2-OG-c by **31** in Figure 4C,D). The analysis used gives an indication of the residual activity, and whether a curve fit to a model with residual activity is better than a model with no residual activity (see refs 48 and 49 for discussion). In the case of the inhibition of 2-OG-c by **31**, the residual activity was found to be 41 ± 7%. Throughout the tables, this type of situation is indicated by adding the maximum inhibition value (i.e., 59% in this case). The pI₅₀ and, hence, the IC₅₀ value in this case represents the IC₅₀ value for the inhibitable portion of the hydrolytic activity. Residual activity has been seen in other situations (such as the inhibition of FAAH activity by *N*-palmitoylethanolamine analogues⁵⁰) and is most probably a reflection of the limited solubility of these very lipophilic compounds. In some cases, this inhibitable portion was less than 50% (such as is seen for the inhibition of 2-OG-m hydrolysis by **16**, where the residual activity was 64 ± 12%, that is, an inhibitable portion of 36%). In other cases, such as the inhibition of 2-OG-c hydrolysis by **16**, the calculated IC₅₀ value was higher than the highest (100 μM) concentration tested (in this case the value was calculated to be 160 μM). Finally, in a few cases, the inhibition was insufficient to fit a meaningful curve. In these cases, the observed inhibition at the 100 μM concentration has been indicated (e.g., 42 ± 6% and 36 ± 3% inhibition of 2-OG-c and 2-OG-m hydrolysis, respectively, by **16**, Table 2).

Differences between Effects upon 2-OG Hydrolysis in Membrane and Soluble Fractions. In general, compounds showed lower potency as inhibitors of 2-OG hydrolysis in

Table 2. Influence of the Fatty Acid Chain^a

Cpd	Fatty acid chain	pI ₅₀ [IC ₅₀ , μM]		
		2-OG-c	2-OG-m	AEA-m
1	C ₅ H ₁₁	5.35±0.05 [4.5]	4.72±0.05 [19]	4.91±0.05 [12]
9		4.97±0.05 [11]	4.30±0.04 [50]	5.80±0.05 [1.6]
10		4.64±0.05 [23]	<4 (18±1%) ^c	5.00±0.03 [10, 94%] ^b
11		<4 (6±4%) ^c	<4 (8±2%) ^c	4.96±0.05 [11]
12		4.87±0.08 [13, 84%] ^b	4.55±0.06 [28] ^b	5.09±0.07 [8.2]

5	C ₅ H ₁₁	5.26±0.04 [5.6]	4.58±0.05 [26]	4.30±0.06 [51]
13		4.64±0.03 [23]	<4 (33±4%) ^c	4.73±0.02 [19]
14		4.1±0.1 [73]	<4 (38±4%) ^c	5.13±0.04 [7.5]
15		<4 (12±7%) ^c	<4 (35±1%) ^c	4.53±0.05 [29]
16		<4 (42±6%) ^c	<4 (36±3%) ^c	5.0±0.1 [10, 82%] ^b

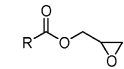
^a For an explanation of the data, see the footnotes for Table 1.

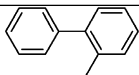
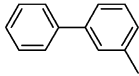
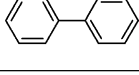
URB597-treated membranes than in cytosolic fractions. There was, however, a variation in the degree of selectivity between the two fractions, ranging from little or none (e.g., **4**) to marked (e.g., **8**, **10**; see Tables 1 and 2). One possible explanation for this selectivity is simply that the compounds are more stable when incubated with the cytosolic fractions than for the membrane fractions. If this was the case, then it would be expected that the potency of the compounds would decrease if they were preincubated with the membranes at 37 °C prior to addition of substrate. This was tested using two compounds, **1** and **5**, and with membrane-bound AEA hydrolysis as the marker of activity (since in our hands FAAH is more thermostable than 2-OG hydrolytic activities). For a concentration of **1** of 10 μM, the observed activity (% of control, means ± sem, *n* = 3) was 65 ± 1, 66 ± 4 and 67 ± 4 following preincubation times of 0, 60, and 120 min, followed by a 4 min AEA incubation time and assay workup, as described previously.⁵¹ No loss of effect following preincubation was seen with concentrations of **1** of 2 and 50 μM and for **5** at concentrations of 10 and 50 μM (data not shown). This would argue that the selectivity of these two compounds for the cytosolic over membrane hydrolytic activities is not due to a stability issue and would further support the suggestion that more than one hydrolytic activity is present in the brain.

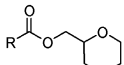
Structure–Activity Relationship Study for Monoacylglycerol Hydrolysis Inhibition. Influence of the Heterocyclic Moiety. Compounds **1–8** (Table 1) are able to inhibit the cytosolic 2-OG hydrolyzing activity, with IC₅₀ values in the low micromolar range (4.5–45 μM; Table 1). Additionally,

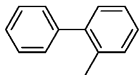
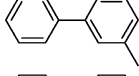
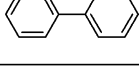
these compounds exhibit a lower inhibitory capacity toward membrane 2-OG hydrolyzing activity. The best profiles were obtained for compounds **1** and **5**. Oxiran-2-ylmethyl (5Z,8Z,11Z,14Z)-icosa-5,8,11,14-tetraenoate (**1**) resulted in the most potent compound toward 2-OG-c hydrolysis (IC₅₀ (**1**) = 4.5 μM), while tetrahydro-2H-pyran-2-ylmethyl (5Z,8Z,11Z,14Z)-icosa-5,8,11,14-tetraenoate (**5**), with IC₅₀ (2-OG-c) = 5.6 μM, was the most selective compound versus FAAH with almost 10-fold selectivity (IC₅₀ (FAAH) = 51 μM). In collaboration with two of us, this compound has also been assessed by Muccioli et al.³⁸ (and given the compound number 40 in their study). That study found that the compound was roughly equipotent toward the metabolism of AEA (in homogenates made from microglial cells) and 2-AG (in homogenates made from neurons),³⁸ which would suggest that the latter is primarily a measure of the 2-OG-m hydrolytic activity seen here. A direct comparison of potencies is difficult because that study used a very much lower substrate concentration (0.8 nM for AEA and 1.25 nM for 2-AG)³⁸ than the 2 μM used here. A competitive mode of action of **5** versus FAAH would predict that the potency in the reported study should be higher than ours. Visual inspection of their data (Figure 2E of ref 38) indicates that this is indeed the case. Compound **16** was also tested (number 38 in Figure 2 of ref 38) and found to be more potent toward the AEA activity than the neuronal 2-AG hydrolytic activity.³⁸ A similar result was seen here (Figure 4C).

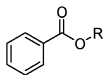
Interestingly, for compounds **1–8**, loss of affinity toward the soluble 2-OG hydrolytic activity correlates with relative increases in FAAH affinity, as occurs with compounds **3** (IC₅₀

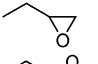
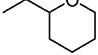
Table 3. Influence of Phenyl and Biphenyl Groups^a


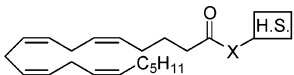
Cpd	R	pI ₅₀ [IC ₅₀ , μM]		
		2-OG-c	2-OG-m	AEA-m
17		<4 (29±3%) ^c	<4 (18±10%) ^c	<4 (5±7%) ^c
18		<4 (40.0±0.6%) ^c	<4 (19±4%) ^c	4.22±0.04 [61]
19		<4 (43±2%) ^c	<4 (9±5%) ^c	4.45±0.04 [35]

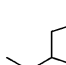
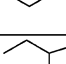
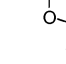
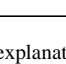


Cpd	R	pI ₅₀ [IC ₅₀ , μM]		
		2-OG-c	2-OG-m	AEA-m
20		<4 (38±3%) ^c	<4 (47±4%) ^c	4.37±0.09 [43]
21		<4 (36±3%) ^c	<4 (49±3%) ^c	4.75±0.04 [18]
22		<4 (43±7%) ^c	4.1±0.2 [80]	4.49±0.04 [32]



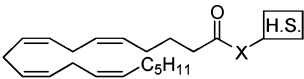
Cpd	R	pI ₅₀ [IC ₅₀ , μM]		
		2-OG-c	2-OG-m	AEA-m
23		<4 (14±5%) ^c	<4 (0.2±7%) ^c	<4 (19±4%) ^c
24		5.5±0.2 [3.0, 53%] ^b	<4 (24±4%) ^c	4.28±0.05 [53]

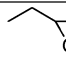
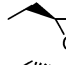

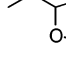
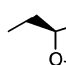
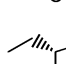
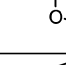
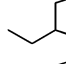
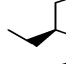
^a For an explanation of the data, see the footnotes for Table 1.**Table 4.** Influence of the Ester Group^a


Cpd	H. S.	X	pI ₅₀ [IC ₅₀ , μM]		
			2-OG-c	2-OG-m	AEA-m
2		O	4.67±0.04 [21]	4.1±0.1 [75]	4.48±0.06 [33]
25		NH	4.47±0.06 [34]	<4 (44±3%) ^c	4.25±0.04 [56]
4		O	4.3±0.1 [45]	4.0±0.1 [95]	4.0±0.1 [98]
26		NH	4.8±0.1 [15, 71%] ^b	<4 (45±1%) ^c	4.05±0.05 [90]

^a For an explanation of the data, see the footnotes for Table 1.

(2-OG-c) = 43 μM and IC₅₀ (FAAH) = 11 μM) and **6** (IC₅₀ (2-OG-c) = 30 μM and IC₅₀ (FAAH) = 5.3 μM). Finally, the decrease in potency observed for compound **8** in all of the three assays suggests the negative influence of increasing the size of the heterocyclic moiety.

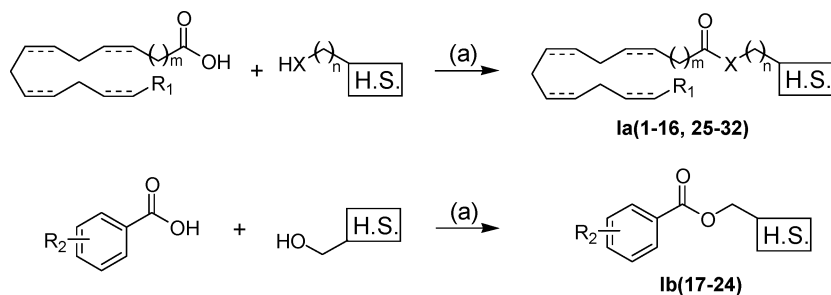
Table 5. Influence of the Stereogenic Center^a


Cpd	H. S.	X	pI ₅₀ [IC ₅₀ , μM]		
			2-OG-c	2-OG-m	AEA-m
1		O	5.35±0.05 [4.5]	4.72±0.05 [19]	4.91±0.05 [12]
27		O	5.2±0.1 [6.3, 68%] ^b	<4 (43±4%) ^c	5.22±0.04 [6.0]
28		O	5.1±0.1 [8.0, 69%] ^b	<4 (47±3%) ^c	4.93±0.04 [12]
4		O	4.3±0.1 [45]	4.0±0.1 [95]	4.0±0.1 [98]
29		O	4.22±0.09 [60]	<4 (34±6%) ^c	4.55±0.06 [28]
30		O	<4 (46±3%) ^c	<4 (38±5%) ^c	4.76±0.05 [17]
25		NH	4.47±0.06 [34]	<4 (44±3%) ^c	4.25±0.04 [56]
31		NH	5.5±0.2 [3.5, 59%] ^b	4.1±0.1 [70]	4.16±0.02 [69]
32		NH	4.59±0.05 [25]	4.09±0.07 [81]	4.01±0.06 [99]

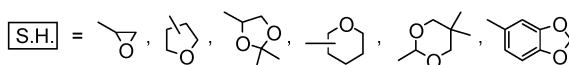
^a For an explanation of the data, see the footnotes for Table 1.

Influence of the Fatty Acid Chain. For the compounds with the best profiles of potency and selectivity (**1** and **5**), we replaced the arachidonic acid moiety for different fatty acid chains, keeping constant the heterocyclic subunit (Table 2, compounds **9–16**). However, none of the modifications yielded any appreciable improvement either in potency or in selectivity. With respect to the oxirane derivatives **9–11**, a decrease in the number of double bonds involves a concomitant reduction in the potency as inhibitors of 2-OG-c hydrolysis, ranging from the initial value of 4.5 μM of the arachidonic acid derivative **1** to no inhibition at 100 μM for compound **11**, the oleic acid analogue. This trend is also appreciable for 2-OG-m hydrolysis, where the IC₅₀ value of 19 μM of compound **1** increases for derivatives with less unsaturations, as seen, for example, for compound **9**, with three double bonds (IC₅₀ = 50 μM), **10**, with two double bonds (18% inhibition at a concentration of 100 μM), or **11**, with one double bond (8% inhibition at a concentration of 100 μM). The same tendency is observed for the 2-tetrahydropyran derivatives, where the progressive elimination of unsaturations brings about a parallel decrease in inhibitory potency toward 2-OG-c hydrolysis, as seen for compounds **13–15** (Table 2), which IC₅₀ values range from 23 μM for compound **13** to a lack of activity of compound **15** (12% inhibition at 100 μM). Likewise, they also decrease their potency toward 2-OG-m hydrolysis from the IC₅₀ of 26 μM of arachidonic acid derivative **5** to a maximal inhibition between 33 and 38% at 100 μM for compounds **13–15**. In both cases, for oxirane and tetrahydropyran derivatives, FAAH inhibition is less sensitive to the variations in the fatty acid chain, showing even slight increases in potency.

With respect to the chain length of the monounsaturated compounds, shortening of the chain from the oleic acid (C-18) derivatives **11** and **15** to their corresponding palmitoleic (C-

Scheme 1. Synthesis of Compounds of General Structure I^a

X = O, NH; R₁ = H, C₂H₅, C₅H₁₁; R₂ = H, Ph; m = 3, 4; n = 0-2



Reagents: (a) DCC, DMAP, CH₂Cl₂, Ar, rt

^a Reagents and conditions: (a) DCC, DMAP, CH₂Cl₂, Ar, rt.

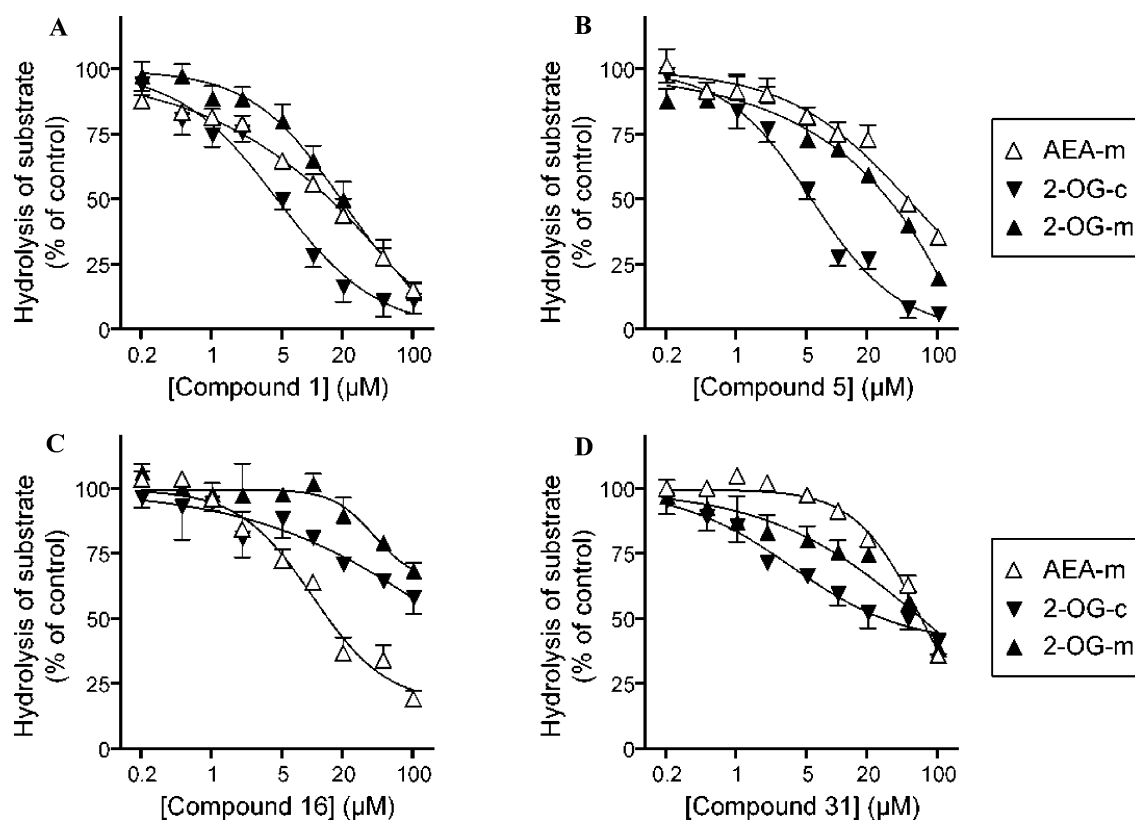


Figure 4. Inhibition of the hydrolysis of AEA and 2-OG by compounds **1** (panel A, $n = 6$), **5** (panel B, $n = 3$), **16** (panel C, $n = 2-3$), and **31** (panel D, $n = 3$).

16) derivatives **12** and **16** improved the affinity of the compounds toward 2-OG-c hydrolysis. Thus, **12** inhibited 2-OG-c hydrolysis, with an IC₅₀ value of 13 μM , whereas **11** was inactive. Similarly, the maximum observed inhibition values were 42% (**16**) versus 12% (for **15**). For the inhibition of 2-OG-m hydrolysis, no consistent change was seen: **11** was inactive, whereas **12** inhibited the hydrolysis with an IC₅₀ value of 28 μM ; **15** and **16** were both weak inhibitors, producing 35 and 36% inhibition of 2-OG-m hydrolysis at 100 μM , respectively. Because none of the acyl side chains gave better results than arachidonic acid, we tried next to restrict the flexible conformation of this chain with the isosteric but more rigid core of the biphenyl group. Thus, we synthesized compounds **17-22** (Table 3). Unfortunately, none of the relative orientations tested (*ortho*-, *meta*-, or *para*-positions) resulted in any ap-

preciable inhibition of the two 2-OG hydrolytic activities, showing very low maximum inhibition values between 9%-49% at 100 μM concentration. Only compound **22** showed a little higher inhibitory capacity but even though with a quite moderate IC₅₀ value of 80 μM toward 2-OG-m hydrolysis. To rule out the existence of steric factors that could hinder the binding in the pocket of the enzyme(s), we eliminated one of the phenyl rings (compounds **23** and **24**). Nonetheless, the inhibitory potency remained low, with little or no inhibition being found for compound **23** and a partial, albeit potent, inhibition of 2-OG-c hydrolysis for the tetrahydropyran derivative **24**.

Influence of the Ester Group. Because none of the surrogates envisioned for replacement of the arachidonic acid chain improved the inhibitory profiles of the initial compounds, we have studied the influence of the ester linkage by substitution

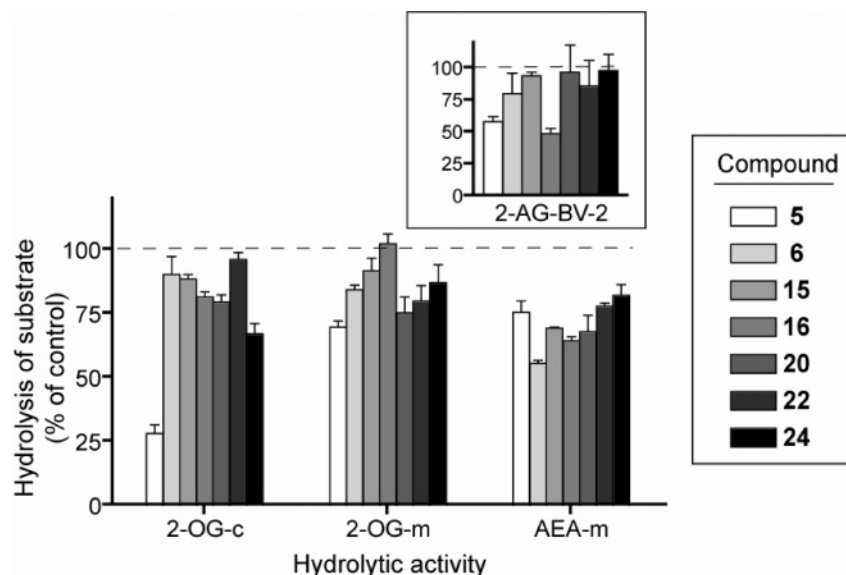


Figure 5. Comparison of the effects of compounds **5**, **6**, **15**, **16**, **20**, **22**, and **24** at a concentration of 10 μM on the hydrolysis of 2-OG by cytosol (2-OG-c) and membrane (2-OG-m) preparations and the hydrolysis of AEA by membrane fractions (AEA-m). For comparative purposes, the inset shows the percentage of hydrolysis of 2-AG in the presence of 10 μM of the same compounds in BV-2 cell homogenates (“2-AG-BV-2”, data taken from ref 38; compounds **5**, **6**, **15**, **16**, **20**, **22**, and **24** shown here correspond to compounds **40**, **44**, **39**, **38**, **42**, **41**, and **43**, respectively, in ref 38).

for an isosteric amide group (Table 4). In general, substitution of the ester group by the amide did not improve potency or selectivity in any consistent manner. Thus, while there was no difference in the potencies for compounds **25** and **2** (IC_{50} values of 34 and 21 μM , respectively), amide **26** was slightly more potent as an inhibitor of 2-OG-c hydrolysis compared to its corresponding ester **4** (IC_{50} values of 15 μM (albeit not with complete inhibition) and 45 μM , respectively). No large changes in potency for FAAH or for 2-OG-m hydrolysis were seen.

Influence of the Stereogenic Center. We have also studied the influence of the stereogenic center in the heterocyclic subunit for some of the representative compounds (Table 5). The stereogenic center does not exert a great influence on inhibition of 2-OG-c hydrolysis, as seen in compounds **27** and **28**, with IC_{50} values for 2-OG-c of 4.5 μM (racemic **1**), 6.3 μM (*R*-enantiomer **27**), and 8.0 μM (*S*-enantiomer **28**). Additional examples with larger oxygenated cycles (**29**–**32**) did not suggest any consistent trend. For example, the *R*-enantiomer **29** is more potent than its *S*-counterpart (IC_{50} (**29**) = 60 μM and maximal inhibition of 100% vs IC_{50} (**30**) > 100 μM and maximal inhibition of 46%), whereas the *S*-enantiomer **32** is more potent than the *R*-derivative **31** (IC_{50} (**32**) = 25 μM and a maximum inhibition of 100% versus IC_{50} (**31**) = 3.5 μM corresponding to a maximum inhibition value of 59%).

Finally, FAAH inhibition is not consistently affected by the stereogenic center, as seen in compound **1** (IC_{50} = 12 μM) versus its enantiomers **27** and **28** (IC_{50} values of 6 and 12 μM , respectively), compound **4** (IC_{50} = 98 μM) versus its enantiomers **29** and **30** (IC_{50} values of 28 and 17 μM , respectively) or **25** (IC_{50} = 56 μM) versus its enantiomers **31** and **32** (IC_{50} values of 69 and 99 μM , respectively).

Comparison of Selected Compounds with Previously Reported Effects upon 2-AG Hydrolysis in BV-2 Cell Homogenates. In supplemental data, Muccioli et al.³⁸ reported the effects of seven of the compounds above at a single concentration (10 μM) with respect to their ability to affect the hydrolysis of 2-AG in homogenates of BV-2 microglial cells. The results can be compared with the corresponding data from our study (Figure 5). It should again be remembered that the substrate concentration in that study (1.25 nM)³⁸ is much lower

than the 2 μM 2-OG used here (chosen to be near the K_m value of 2.2 μM , which we have previously reported for 2-OG hydrolysis by cytosolic fractions⁴¹). The authors also used 2-AG rather than 2-OG. However, potencies of the compounds relative to each other within a given assay can be compared. These are shown in Figure 5, where it can be seen that for 2-OG-c, **5** is the only compound with a robust effect at the concentration of 10 μM , whereas for the microglial cell data (“2-AG-BV-2”),³⁸ both **5** and **16** have pronounced effects. None of the compounds stand out for 2-OG-m, indicating that the pharmacological properties of the 2-AG hydrolytic activity in the microglial cells are different to both cytosolic and membrane bound 2-OG hydrolytic activities for the rat cerebellum.

Discussion

These data represent the first systematic SAR described for inhibition of monoacylglycerol hydrolysis by brain cytosolic and particulate fractions. The two best inhibitory profiles of our series were obtained for compounds **1** and **5**, being oxiran-2-ylmethyl (5*Z*,8*Z*,11*Z*,14*Z*)-icosa-5,8,11,14-tetraenoate (**1**), the most potent of the compounds causing complete inhibition of 2-OG hydrolysis by the cytosolic fractions (IC_{50} (**1**) = 4.5 μM), and tetrahydro-2*H*-pyran-2-ylmethyl (5*Z*,8*Z*,11*Z*,14*Z*)-icosa-5,8,11,14-tetraenoate (**5**), the most selective for cytosolic 2-OG hydrolysis versus FAAH ($\text{IC}_{50}\text{FAAH}/\text{IC}_{50}$ 2-OG-s \approx 10). Compound **1** is as potent as the best compounds emanating from a previous study,⁴² the α -methyl analogues of the 20:3 and 22:4 homologues of 1-AG, with IC_{50} values of 4.2 and 5.8 μM , respectively. These compounds, however, were not selective vis à vis 2-OG-m or FAAH.⁴² Arachidonoyl-, oleoyl-, and palmitoyl-trifluoromethylketones also inhibit 2-OG-s in the low micromolar range, but all three are considerably more potent as inhibitors of FAAH⁴¹ and can inhibit other enzymes such as phospholipase A₂. The only compound (other than the nonselective compound methylarachidonylfluorophosphate^{26,37,40}) inhibiting 2-AG/2-OG hydrolysis in the submicromolar range is *N*-arachidonylmaleimide (IC_{50} = 140 nM),³⁴ but nothing has yet been published about its selectivity toward FAAH, DAGL, or other proteins with available cysteine residues with whom it may react.

One of the most interesting results of our study is the different inhibition profiles for the cytosolic and membrane bound 2-OG hydrolytic activities, which indicates that they can be distinguished pharmacologically, as well as biochemically in terms of their pH profiles.⁴¹ Whether this reflects different properties of MGL in the different locations, or a different enzymatic composition of the fractions, awaits elucidation. Characterization of the different monoacylglycerol hydrolyzing activities and determination of their physiological relevance is of paramount importance to validate these metabolic pathways as suitable therapeutic targets. Thus, it is critical to establish whether it is therapeutically relevant (and pharmacologically feasible) the inhibition of only particular 2-AG hydrolyzing activities or if complete inhibition is preferable. Regarding selectivity, FAAH stands out as the first obvious target to screen against. Development of selective inhibitors for 2-AG versus AEA hydrolysis has been a long-sought objective because it will allow to determine which is the specific contribution of AEA and 2-AG to those physiological functions where endocannabinoid involvement has been described. Moreover, availability of such compounds will guide the future design of new drugs. Depending on the precise involvement of FAAH and MGL to the pathology under treatment, development of the most suitable drug (either pure or mixed FAAH/MGL inhibitors) will ensure the optimal therapeutic efficiency without producing other undesirable side effects. A second interesting selectivity issue is related to DAGLs α and β , recently described as main contributors to the biosynthesis of 2-AG.³⁵ Considering that these enzymes share some structural properties with MGL (they both are serine hydrolases and show sensitivity toward free sulfhydryl group-modifying agents),³⁵ it is possible that some compounds could inhibit both MGL and DAGL α (as it is the case, for example, for fluorophosphonate UP101, with IC₅₀ values of 3.7 μ M for DAGL α and 3.2 μ M for MGL).⁵² However, two points should be taken into account. First, the compounds analyzed here mimic the structure of 2-AG, which we think is the base of their inhibition toward MGL, and cloned DAGL lacks any appreciable MGL activity.³⁵ Also, if this is the case and they are behaving like 2-AG, we would not expect higher inhibition than the one directly caused by 2-AG as final product. Finally, it is conceivable that under DAGL inhibition the alternative pathways for 2-AG biosynthesis (such as those mediated by phospholipases A1 and C or a phosphatase)²⁵ would undertake the synthesis of 2-AG. Regardless of these considerations, it is clear that DAGLs constitute an interesting target to be taken into account when screening selectivity of MGL inhibitors but especially for future second generation inhibitors that show higher potencies as MGL inhibitors (i.e., IC₅₀ values in the nanomolar range) and optimal selectivity over FAAH.

Conclusions

A series of 2-AG analogues wherein its glycerol moiety was mimicked by different oxygenated heterocycles was prepared and evaluated for MGL activity inhibitory potency as well as selectivity versus FAAH. Different heterocycles, hydrophobic moieties, and variations in the linker between these two subunits have been explored. Notably, some of the synthesized compounds inhibit the completion of 2-OG hydrolysis, showing IC₅₀ values in the low micromolar range. These compounds have allowed us to carry out the first systematic SAR in MGL activity and, in particular, compounds **1** and **5**, the most potent (IC₅₀ (**1**) = 4.5 μ M) and selective versus FAAH (IC₅₀ (**5**, FAAH)/IC₅₀ (**5**, 2-OG-s) \approx 10), respectively, may represent useful tools

that will facilitate the study of the (patho)physiological roles of 2-AG as well as the therapeutic possibilities of MGL inhibition.

Experimental Section

Chemistry. Infrared (IR) spectra were determined on a Perkin-Elmer 781 or Shimadzu-8300 infrared spectrophotometer. Optical rotation [α] was measured using a Perkin-Elmer 781 polarimeter. ¹H and ¹³C NMR spectra were recorded on a Varian VXR-300S, Bruker Avance 3000-AM, or Bruker 200-AC instrument at room temperature (rt) unless stated otherwise. Chemical shifts (δ) are expressed in parts per million relative to internal tetramethylsilane; coupling constants (J) are in hertz. Satisfactory elemental analyses were obtained for all the newly synthesized analogs and are within \pm 0.4% of the theoretical values. Thin-layer chromatography (TLC) was run on Merck silica gel 60 F-254 plates. For normal pressure chromatography, Merck silica gel type 60 (size 70–230) was used. Unless stated otherwise, starting materials used were high-grade commercial products from Aldrich, Acros, Fluka, Merck, or Panreac except arachidonic acid (90% of purity), which was purchased from Sigma.

General Procedure For The Synthesis Of Derivatives 1–32.

To a stirred solution of 1 equiv (100 mg) of carboxylic acid in dry dichloromethane (0.82 mL/mmol) and the appropriate alcohol or amine (5 equiv) in dry dichloromethane (0.27 mL/mmol) in ice bath under argon, a solution of DCC (1 equiv) and DMAP (0.068 equiv) in dry dichloromethane (1.9 mL/mmol) was added dropwise. The mixture was stirred for 5 min at this temperature and then removed from the cooling bath and stirred at room temperature (3–6 h) until no further evolution was observed by TLC. The dicyclohexylurea was filtered off, and the filtrate was washed with saturated NaHCO₃ and, in the case of amides, with 0.5 M HCl. The organic extracts were dried over anhydrous Na₂SO₄. Then the solvent was evaporated under reduced pressure, and the product was purified by column chromatography on silica gel using the appropriate eluent. Compounds **2**, **3**, and **25** showed spectroscopic data identical to those reported previously in the literature.⁵³

(\pm)-Oxiran-2-ylmethyl (5Z,8Z,11Z,14Z)-Icosa-5,8,11,14-tetraenoate (**1**). Yield: 42%. R_f = 0.68 in hexane/chloroform (3:7). IR (CHCl₃, cm⁻¹): 1377, 1418, 1456, 1738, 2860, 2930, 2955, 3014. ¹H NMR (CDCl₃, δ): 0.88 (t, J = 6.8 Hz, 3H, H₂₀); 1.18–1.43 (m, 6H, H₁₇, H₁₈, H₁₉); 1.72 (qt, J = 7.1 Hz, 2H, H₃); 2.00–2.17 (m, 4H, H₄, H₁₆); 2.37 (t, J = 7.6 Hz, 2H, H₂); 2.64 (dd, J = 4.9; 2.7 Hz, 1H, 1H oxirane); 2.78–2.86 (m, 7H, H₇, H₁₀, H₁₂, 1H oxirane); 3.16–3.24 (m, 1H, 1H oxirane); 3.91 (dd, J = 12.2; 6.3 Hz, 1H, 1H₁"); 4.41 (dd, J = 12.2; 2.9 Hz, 1H, 1H₁"); 5.26–5.47 (m, 8H, vinylic-H). ¹³C NMR (CDCl₃, δ): 14.2; 22.7; 24.8; 25.7 (3C); 26.6; 27.3; 29.4; 31.6; 33.5; 44.8; 49.4; 64.9; 127.5; 127.8; 128.1; 128.2; 128.6; 128.8; 129.0; 130.5; 173.4. Chromatography in hexane/chloroform (1:9).

(\pm)-2,2-Dimethyl-1,3-dioxolan-4-ylmethyl (5Z,8Z,11Z,14Z)-Icosa-5,8,11,14-tetraenoate (**4**). Yield: 60%. R_f = 0.42 in chloroform. IR (CHCl₃, cm⁻¹): 1030, 1113, 1416, 1450, 1735, 2833, 2945. ¹H NMR (CDCl₃, δ): 0.88 (t, J = 6.8 Hz, 3H, H₂₀); 1.26–1.32 (m, 6H, H₁₇, H₁₈, H₁₉); 1.37 (s, 3H, CH₃); 1.43 (s, 3H, CH₃); 1.71 (qt, J = 7.3 Hz, 2H, H₃); 2.00–2.16 (m, 4H, H₄, H₁₆); 2.36 (t, J = 7.3 Hz, 2H, H₂); 2.78–2.86 (m, 6H, H₇, H₁₀, H₁₃); 3.73 (dd, J = 8.3; 6.1 Hz, 1H, 1H dioxolane); 4.04–4.15 (m, 3H, 1H₁", 2H dioxolane); 4.19–4.37 (m, 1H, 1H₁"); 5.23–5.40 (m, 8H, vinylic-H). ¹³C NMR (CDCl₃, δ): 14.1; 22.5; 24.7; 25.4; 25.6 (3C); 26.5; 26.7; 27.2; 29.3; 31.5; 33.4; 64.6; 66.4; 73.7; 109.8; 127.5; 127.8; 128.1; 128.2; 128.6; 128.8; 129.0; 130.5; 173.4. Chromatography in hexane/chloroform (3:7).

(\pm)-Tetrahydro-2H-pyran-2-ylmethyl (5Z,8Z,11Z,14Z)-Icosa-5,8,11,14-tetraenoate (**5**). Yield: 29%. R_f = 0.49 in chloroform. IR (CHCl₃, cm⁻¹): 1558, 1653, 1684, 1718, 2934, 3018. ¹H NMR (CDCl₃, δ): 0.89 (t, J = 6.6 Hz, 3H, H₂₀); 1.25–1.40 (m, 6H, H₁₇, H₁₈, H₁₉); 1.49–1.58 (m, 5H, 5H tetrahydropyran); 1.71 (qt, J = 7.3 Hz, 2H, H₃); 1.82–1.90 (m, 1H, 1H tetrahydropyran); 2.01–2.16 (m, 4H, H₄, H₁₆); 2.37 (t, J = 7.5 Hz, 2H, H₂); 2.78–2.86

(m, 6H, H₇, H₁₀, H₁₃); 3.37–3.59 (m, 2H, 2H tetrahydropyran); 3.96–4.13 (m, 3H, H₁'', 1H tetrahydropyran); 5.23–5.37 (m, 8H, vinylic-H). ¹³C NMR (CDCl₃, δ): 14.0; 22.6; 23.0; 24.8; 25.6 (3C); 25.7; 26.6; 27.2; 27.9; 29.3; 31.5; 33.6; 67.3; 68.4; 75.5; 127.5; 127.9; 128.2; 128.6; 128.8 (2C); 129.0; 130.5; 173.5. Chromatography in hexane/ethyl acetate (9:1).

Tetrahydro-2H-pyran-4-yl (5Z,8Z,11Z,14Z)-Icosa-5,8,11,14-tetraenoate (6). Yield: 23%. *R*_f = 0.51 in chloroform. IR (CHCl₃, cm⁻¹): 1362, 1456, 1558, 1653, 1684, 1716, 2933, 3018. ¹H NMR (CDCl₃, δ): 0.89 (t, *J* = 6.6 Hz, 3H, H₂₀); 1.22–1.39 (m, 6H, H₁₇, H₁₈, H₁₉); 1.57–1.78 (m, 4H, H₃, 2H tetrahydropyran); 1.85–1.95 (m, 2H, 2H tetrahydropyran); 2.00–2.17 (m, 4H, H₄, H₁₆); 2.32 (t, *J* = 7.5 Hz, 2H, H₂); 2.78–2.86 (m, 6H, H₇, H₁₀, H₁₃); 3.47–3.59 (m, 2H, 2H tetrahydropyran); 3.86–3.96 (m, 2H, 2H tetrahydropyran); 4.95 (sept, *J* = 4.3 Hz, 1H, C–H–O tetrahydropyran); 5.27–5.47 (m, 8H, vinylic-H). ¹³C NMR (CDCl₃, δ): 14.2; 22.7; 25.0; 25.8 (3C); 26.7; 27.4; 29.5; 31.7; 32.0 (2C); 34.1; 65.5; 69.1; 76.5; 127.7; 128.0; 128.3; 128.4; 128.7; 129.0 (2C); 130.7; 173.4. Chromatography in hexane/ethyl acetate (9:1).

2-(5,5-Dimethyl-1,3-dioxan-2-yl)ethyl (5Z,8Z,11Z,14Z)-Icosa-5,8,11,14-tetraenoate (7). Yield: 41%. *R*_f = 0.40 in chloroform. IR (CHCl₃, cm⁻¹): 1094, 1456, 1472, 1732. ¹H NMR (CDCl₃, δ): 0.72 (s, 3H, CH₃); 0.89 (t, *J* = 6.8 Hz, 3H, H₂₀); 1.18 (s, 3H, CH₃); 1.23–1.43 (m, 6H, H₁₇, H₁₈, H₁₉); 1.70 (qt, *J* = 7.3 Hz, 2H, H₃); 1.96 (q, 2H, *J* = 6.6 Hz, H₂''); 2.04–2.17 (m, 4H, H₄, H₁₆); 2.31 (t, *J* = 7.3 Hz, 2H, H₂); 2.78–2.86 (m, 6H, H₇, H₁₀, H₁₃); 3.41 (d, *J* = 10.5 Hz, 2H, 2H dioxane); 3.60 (d, *J* = 11.0 Hz, 2H, 2H dioxane); 4.20 (t, *J* = 6.6 Hz, 2H, H₁''); 4.53 (t, *J* = 5.1 Hz, 1H, 1H dioxane); 5.26–5.46 (m, 8H, vinylic-H). ¹³C NMR (CDCl₃, δ): 14.0; 21.8; 22.6; 22.9; 24.8; 25.6 (3C); 26.6; 27.2; 29.3; 30.1; 31.5; 33.7; 34.1; 60.0; 77.2 (2C); 99.4; 127.5; 127.9; 128.1; 128.2; 128.6; 128.8; 129.0; 130.5; 173.4. Chromatography in chloroform.

1,3-Benzodioxol-5-ylmethyl (5Z,8Z,11Z,14Z)-Icosa-5,8,11,14-tetraenoate (8). Yield: 74%. *R*_f = 0.35 in hexane/dichloromethane (1:1). IR (CHCl₃, cm⁻¹): 1447, 1491, 1504, 1728, 2930, 2959, 3016. ¹H NMR (CDCl₃, δ): 0.81 (t, *J* = 6.6 Hz, 3H, H₂₀); 1.18–1.32 (m, 6H, H₁₇, H₁₈, H₁₉); 1.64 (qt, *J* = 7.4 Hz, 2H, H₃); 1.93–2.08 (m, 4H, H₄, H₁₆); 2.28 (t, *J* = 7.5 Hz, 2H, H₂); 2.68–2.76 (m, 6H, H₇, H₁₀, H₁₃); 4.94 (s, 2H, H₁''); 5.20–5.37 (m, 8H, vinylic-H); 5.89 (s, 2H, O–CH₂–O); 6.68–6.78 (m, 3H, Ar). ¹³C NMR (CDCl₃, δ): 14.5; 23.0; 25.2 (2C); 26.0; 27.0; 27.6; 29.4; 29.7; 31.9; 34.1; 66.5; 101.6; 108.6; 109.4; 122.7; 127.9; 128.3; 128.5; 128.6; 129.0; 129.3 (2C); 130.2; 130.9; 148.0; 148.2; 173.8. Chromatography in hexane/dichloromethane (1:1).

(±)-Oxiran-2-ylmethyl (9Z,12Z,15Z)-Octadeca-9,12,15-trienoate (9). Yield: 19%. *R*_f = 0.67 in chloroform. IR (CHCl₃, cm⁻¹): 1653, 1732, 2858, 2933, 3020. ¹H NMR (CDCl₃, δ): 0.98 (t, *J* = 7.5 Hz, 3H, H₁₈); 1.25–1.31 (m, 8H, H₄, H₅, H₆, H₇); 1.60–1.67 (m, 2H, H₃); 2.01–2.21 (m, 4H, H₈, H₁₇); 2.36 (t, *J* = 7.6 Hz, 2H, H₂); 2.58 (dd, *J* = 4.9; 2.6 Hz, 1H, 1H oxirane); 2.78–2.87 (m, 5H, H₁₁, H₁₄, 1H oxirane); 3.17–3.26 (m, 1H, 1H oxirane); 3.91 (dd, *J* = 12.2; 5.8 Hz, 1H, 1H₁''); 4.42 (dd, *J* = 12.2; 2.9 Hz, 1H, 1H₁''); 5.25–5.46 (m, 6H, vinylic-H). ¹³C NMR (CDCl₃, δ): 14.3; 20.6; 24.9; 25.5; 25.6 (2C); 27.2; 29.1; 29.2; 29.6; 34.1; 44.7; 49.4; 64.8; 127.1; 127.8; 128.3 (2C); 130.3; 132.0; 183.0. Chromatography in hexane/dichloromethane (2:8).

(±)-Oxiran-2-ylmethyl (9Z,12Z)-Octadeca-9,12-dienoate (10). Yield: 36%. *R*_f = 0.30 in dichloromethane. IR (CHCl₃, cm⁻¹): 1379, 1437, 1460, 1732, 2858, 2932. ¹H NMR (CDCl₃, δ): 0.88 (t, *J* = 6.5 Hz, 3H, H₁₈); 1.18–1.35 (m, 14H, H_{4–7}, H_{15–17}); 1.60–1.67 (m, 2H, H₃); 2.00–2.06 (m, 4H, H₈, H₁₄); 2.35 (t, *J* = 7.3 Hz, 2H, H₂); 2.65 (dd, *J* = 4.9; 2.6 Hz, 1H, 1H oxirane); 2.77 (t, *J* = 5.7 Hz, 2H, H₁₁); 2.82–2.87 (m, 1H, 1H oxirane); 3.17–3.25 (m, 1H, 1H oxirane); 3.90 (dd, *J* = 12.3; 6.3 Hz, 1H, 1H₁''); 4.41 (dd, *J* = 12.3; 3.0 Hz, 1H, 1H₁''); 5.25–5.45 (m, 4H, vinylic-H). ¹³C NMR (CDCl₃, δ): 14.2; 22.7; 24.9; 25.7; 27.3 (2C); 29.2 (3C); 29.4; 29.7; 31.6; 34.2; 44.7; 49.5; 64.8; 128.0; 128.1; 130.1; 130.3; 173.6. Chromatography in hexane/dichloromethane (2:8).

(±)-Oxiran-2-ylmethyl (9Z)-Octadec-9-enoate (11). Yield: 33%. *R*_f = 0.51 in chloroform. IR (CHCl₃, cm⁻¹): 1456, 1558, 1653, 1734, 2856, 2928, 3018. ¹H NMR (CDCl₃, δ): 0.81 (t, *J* =

6.7 Hz, 3H, H₁₈); 1.15–1.24 (m, 20H, H_{4–7}, H_{12–17}); 1.53–1.57 (m, 2H, H₃); 1.89–1.96 (m, 4H, H₈, H₁₁); 2.28 (t, *J* = 7.3 Hz, 2H, H₂); 2.58 (dd, *J* = 4.9; 2.6 Hz, 1H, 1H oxirane); 2.78 (t, *J* = 4.9 Hz, 1H, 1H oxirane); 3.12–3.15 (m, 1H, 1H oxirane); 3.84 (dd, *J* = 12.3; 6.3 Hz, 1H, 1H₁''); 4.35 (dd, *J* = 12.3; 3.0 Hz, 1H, 1H₁''); 5.25–5.31 (m, 2H, vinylic-H). ¹³C NMR (CDCl₃, δ): 14.1; 22.6; 24.8; 27.1; 27.2; 29.1 (3C); 29.3 (2C); 29.5; 29.6; 29.7; 31.9; 34.0; 44.6; 49.3; 64.7; 129.7; 130.0; 173.1. Chromatography in hexane/ethyl acetate (9:1).

(±)-Oxiran-2-ylmethyl (9Z)-Hexadec-9-enoate (12). Yield: 25%. *R*_f = 0.50 in chloroform. IR (CHCl₃, cm⁻¹): 1551, 1743, 2856, 2928. ¹H NMR (CDCl₃, δ): 0.88 (t, *J* = 6.8 Hz, 3H, H₁₆); 1.28–1.30 (m, 16H, H_{4–7}, H_{12–15}); 1.59–1.67 (m, 2H, H₃); 1.99–2.02 (m, 4H, H₈, H₁₁); 2.35 (t, *J* = 7.1 Hz, 2H, H₂); 2.63 (dd, *J* = 4.9; 2.4 Hz, 1H, 1H oxirane); 2.84 (dd, *J* = 4.9; 4.2 Hz, 1H, 1H oxirane); 3.16–3.24 (m, 1H, 1H oxirane); 3.90 (dd, *J* = 12.2; 6.3 Hz, 1H, 1H₁''); 4.41 (dd, *J* = 12.3; 3.2 Hz, 1H, 1H₁''); 5.26–5.37 (m, 2H, vinylic-H). ¹³C NMR (CDCl₃, δ): 14.0; 22.6; 24.8; 27.1; 27.2; 28.9; 29.0 (2C); 29.1; 29.6; 29.7; 31.7; 34.0; 44.6; 49.3; 64.7; 129.7; 130.0; 173.5. Chromatography in hexane/chloroform (2:8).

(±)-Tetrahydro-2H-pyran-2-ylmethyl (9Z,12Z,15Z)-Octadeca-9,12,15-trienoate (13). Yield: 55%. *R*_f = 0.20 in hexane/chloroform (2:8). IR (CHCl₃, cm⁻¹): 1558, 1732, 2856, 2935, 3016. ¹H NMR (CDCl₃, δ): 0.90 (t, *J* = 7.5 Hz, 3H, H₁₈); 1.23–1.42 (m, 10H, H_{4–7}, 2H tetrahydropyran); 1.46–1.67 (m, 5H, H₃, 3H tetrahydropyran); 1.80–1.91 (m, 1H, 1H tetrahydropyran); 1.94–2.08 (m, 4H, H₈, H₁₇); 2.28 (t, *J* = 7.5 Hz, 2H, H₂); 2.71–2.76 (m, 4H, H₁₁, H₁₄); 3.31–3.49 (m, 2H, 2H tetrahydropyran); 3.88–4.06 (m, 3H, H₁'', 1H tetrahydropyran); 5.18–5.39 (m, 6H, vinylic-H). ¹³C NMR (CDCl₃, δ): 14.3; 20.6; 23.0; 25.0; 25.5; 25.6; 25.8; 27.2; 27.9; 29.1 (2C); 29.2; 29.6; 34.2; 67.3; 68.4; 75.5; 127.1; 127.7; 128.3 (2C); 130.3; 132.0; 173.9. Chromatography in hexane/chloroform (2:8).

(±)-Tetrahydro-2H-pyran-2-ylmethyl (9Z,12Z)-Octadeca-9,12-dienoate (14). Yield: 44%. *R*_f = 0.12 in hexane/chloroform (1:1). IR (CHCl₃, cm⁻¹): 1558, 1653, 1734, 2856, 2930, 3018. ¹H NMR (CDCl₃, δ): 0.82 (t, *J* = 6.7 Hz, 3H, H₁₈); 1.09–1.32 (m, 16H, H_{4–7}, H_{15–17}, 2H tetrahydropyran); 1.40–1.61 (m, 5H, H₃, 3H tetrahydropyran); 1.77–1.82 (m, 1H, 1H tetrahydropyran); 1.93–1.99 (m, 4H, H₈, H₁₄); 2.28 (t, *J* = 7.3 Hz, 2H, H₂); 2.70 (t, *J* = 5.7 Hz, 2H, H₁₁); 3.31–3.49 (m, 2H, 2H tetrahydropyran); 3.88–4.06 (m, 3H, H₁'', 1H tetrahydropyran); 5.19–5.31 (m, 4H, vinylic-H). ¹³C NMR (CDCl₃, δ): 14.0; 22.5; 23.0; 24.9; 25.6; 25.7; 27.2 (2C); 27.8; 29.1 (2C); 29.2; 29.3; 29.6; 31.5; 34.2; 67.2; 68.4; 75.5; 127.9; 128.0; 130.0; 130.2; 173.8. Chromatography in hexane/chloroform (1:1).

(±)-Tetrahydro-2H-pyran-2-ylmethyl (9Z)-Octadec-9-enoate (15). Yield: 91%. *R*_f = 0.13 in hexane/chloroform (1:1). IR (CHCl₃, cm⁻¹): 1558, 1734, 2928, 3018. ¹H NMR (CDCl₃, δ): 0.81 (t, *J* = 6.7 Hz, 3H, H₁₈); 1.18–1.24 (m, 22H, H_{4–7}, H_{12–17}, 2H tetrahydropyran); 1.39–1.55 (m, 5H, H₃, 3H tetrahydropyran); 1.77–1.82 (m, 1H, 1H tetrahydropyran); 1.92–1.98 (m, 4H, H₈, H₁₁); 2.28 (t, *J* = 7.3 Hz, 2H, H₂); 3.31–3.49 (m, 2H, 2H tetrahydropyran); 3.88–4.06 (m, 3H, H₁'', 1H tetrahydropyran); 5.20–5.36 (m, 2H, vinylic-H). ¹³C NMR (CDCl₃, δ): 14.2; 22.8; 23.1; 25.0; 25.9; 27.3; 27.4; 28.0; 29.2 (2C); 29.3 (2C); 29.4; 29.7; 29.8; 29.9; 32.0; 34.3; 67.4; 68.5; 75.6; 129.9; 130.1; 174.0. Chromatography in hexane/chloroform (1:1).

(±)-Tetrahydro-2H-pyran-2-ylmethyl (9Z)-Hexadec-9-enoate (16). Yield: 69%. *R*_f = 0.10 in hexane/chloroform (1:1). IR (CHCl₃, cm⁻¹): 1558, 1734, 2930, 3018. ¹H NMR (CDCl₃, δ): 0.81 (t, *J* = 6.7 Hz, 3H, H₁₆); 1.18–1.34 (m, 18H, H_{4–7}, H_{12–15}, 2H tetrahydropyran); 1.40–1.58 (m, 5H, H₃, 3H tetrahydropyran); 1.77–1.82 (m, 1H, 1H tetrahydropyran); 1.85–2.03 (m, 4H, H₈, H₁₁); 2.28 (t, *J* = 7.3 Hz, 2H, H₂); 3.31–3.52 (m, 2H, 2H tetrahydropyran); 3.88–4.06 (m, 3H, H₁'', 1H tetrahydropyran); 5.19–5.35 (m, 2H, vinylic-H). ¹³C NMR (CDCl₃, δ): 14.1; 22.6; 23.0; 25.0; 25.8; 27.2 (2C); 27.9; 29.0; 29.1 (2C); 29.2; 29.7; 29.8; 31.8; 34.2; 67.3; 68.4; 75.5; 129.8; 130.0; 173.9. Chromatography in hexane/chloroform (1:1).

(±)-**Oxiran-2-ylmethyl 1,1'-Biphenyl-2-carboxylate (17)**. Yield: 27%. $R_f = 0.33$ in chloroform. IR (CHCl₃, cm⁻¹): 1344, 1418, 1452, 1506, 1720, 2932, 2974. ¹H NMR (CDCl₃, δ): 2.32 (dd, $J = 4.9$; 2.6 Hz, 1H, 1H oxirane); 2.60 (ap t, $J = 4.8$ Hz, 1H, 1H oxirane); 2.78–2.86 (m, 1H, 1H oxirane); 3.89 (dd, $J = 12.2$; 5.8 Hz, 1H, 1H₁''); 4.20 (dd, $J = 12.2$; 3.6 Hz, 1H, 1H₁''); 7.23–7.40 (m, 7H, Ar); 7.46–7.50 (m, 1H, Ar); 7.80 (dd, $J = 7.5$; 1.4 Hz, 1H, Ar). ¹³C NMR (CDCl₃, δ): 44.5; 48.7; 65.2; 127.0; 127.1; 127.9 (2C); 128.2 (2C); 129.9; 130.2; 130.6; 131.4; 141.3; 142.6; 168.2. Chromatography in chloroform.

(±)-**Oxiran-2-ylmethyl 1,1'-Biphenyl-3-carboxylate (18)**. Yield: 24%. $R_f = 0.38$ in hexane/dichloromethane (1:9). IR (CHCl₃, cm⁻¹): 1304, 1346, 1587, 1601, 1717, 3020. ¹H NMR (CDCl₃, δ): 2.67 (dd, $J = 4.8$; 2.6 Hz, 1H, 1H oxirane); 2.84 (ap t, $J = 4.7$ Hz, 1H, 1H oxirane); 3.26–3.34 (m, 1H, 1H oxirane); 4.13 (dd, $J = 12.3$; 6.3 Hz, 1H, 1H₁''); 4.62 (dd, $J = 12.3$; 3.1 Hz, 1H, 1H₁''); 7.30–7.38 (m, 6H, Ar); 7.70–7.75 (m, 1H, Ar); 7.95–7.99 (m, 1H, Ar); 8.21–8.25 (m, 1H, Ar). ¹³C NMR (CDCl₃, δ): 44.7; 49.4; 65.5; 127.1 (2C); 127.7; 128.3; 128.4; 128.8 (3C); 130.1; 131.8; 140.0; 141.5; 166.2. Chromatography in hexane/dichloromethane (1:9).

(±)-**Oxiran-2-ylmethyl 1,1'-Biphenyl-4-carboxylate (19)**. Yield: 35%. $R_f = 0.32$ in chloroform. IR (CHCl₃, cm⁻¹): 1312, 1448, 1609, 1717, 3018. ¹H NMR (CDCl₃, δ): 2.69 (dd, $J = 4.8$; 2.6 Hz, 1H, 1H oxirane); 2.85 (ap t, $J = 4.6$ Hz, 1H, 1H oxirane); 3.26–3.34 (m, 1H, 1H oxirane); 4.12 (dd, $J = 12.3$; 6.3 Hz, 1H, 1H₁''); 4.62 (dd, $J = 12.3$; 3.0 Hz, 1H, 1H₁''); 7.30–7.46 (m, 3H, Ar); 7.55–7.63 (m, 4H, Ar); 8.08 (d, $J = 8.3$ Hz, 2H, Ar). ¹³C NMR (CDCl₃, δ): 44.6; 49.4; 65.3; 127.0 (2C); 127.2 (2C); 128.1; 128.3; 128.8 (2C); 130.2 (2C); 139.8; 145.8; 166.0. Chromatography in chloroform.

(±)-**Tetrahydro-2H-pyran-2-ylmethyl 1,1'-Biphenyl-2-carboxylate (20)**. Yield: 61%. $R_f = 0.40$ in chloroform. IR (CHCl₃, cm⁻¹): 1452, 1724, 2939. ¹H NMR (CDCl₃, δ): 0.94–1.08 (m, 1H, 1H tetrahydropyran); 1.18–1.29 (m, 1H, 1H tetrahydropyran); 1.32–1.43 (m, 3H, 3H tetrahydropyran); 1.52–1.67 (m, 1H, 1H tetrahydropyran); 3.06–3.30 (m, 2H, 2H tetrahydropyran); 3.81–3.96 (m, 3H, H₁'', 1H tetrahydropyran); 7.24–7.49 (m, 8H, Ar); 7.77 (dd, $J = 7.7$; 1.4 Hz, 1H, Ar). ¹³C NMR (CDCl₃, δ): 23.0; 25.8; 27.9; 68.0; 68.4; 75.2; 127.2 (2C); 128.2 (2C); 128.6 (2C); 130.1; 130.8; 131.1; 131.3; 141.7; 142.6; 168.8. Chromatography in hexane/chloroform (2:8).

(±)-**Tetrahydro-2H-pyran-2-ylmethyl 1,1'-Biphenyl-3-carboxylate (21)**. Yield: 45%. $R_f = 0.43$ in chloroform. IR (CHCl₃, cm⁻¹): 1049, 1310, 1423, 1716, 2943. ¹H NMR (CDCl₃, δ): 1.35–1.66 (m, 5H, 5H tetrahydropyran); 1.89–1.92 (m, 1H, 1H tetrahydropyran); 3.42–3.54 (m, 1H, 1H tetrahydropyran); 3.66–3.76 (m, 1H, 1H tetrahydropyran); 3.91–4.15 (m, 1H, 1H tetrahydropyran); 4.32–4.38 (m, 2H, H₁''); 7.34–7.65 (m, 6H, Ar); 7.78 (dt, $J = 7.7$; 1.8 Hz, 1H, Ar); 8.05 (dt, $J = 7.7$; 1.8 Hz, 1H, Ar); 8.30 (t, $J = 1.8$ Hz, 1H, Ar). ¹³C NMR (CDCl₃, δ): 23.0; 25.8; 28.1; 68.0; 68.4; 75.5; 127.2 (2C); 127.7; 128.4; 128.5; 128.8; 128.9 (2C); 130.7; 131.6; 140.2; 141.4; 166.5. Chromatography in dichloromethane.

(±)-**Tetrahydro-2H-pyran-2-ylmethyl 1,1'-Biphenyl-4-carboxylate (22)**. Yield: 61%. $R_f = 0.39$ in hexane/chloroform (2:8). IR (CHCl₃, cm⁻¹): 1610, 1711, 2943. ¹H NMR (CDCl₃, δ): 1.36–1.71 (m, 5H, 5H tetrahydropyran); 1.90–1.93 (m, 1H, 1H tetrahydropyran); 3.35–3.48 (m, 1H, 1H tetrahydropyran); 3.66–3.76 (m, 1H, 1H tetrahydropyran); 4.01–4.09 (m, 1H, 1H tetrahydropyran); 4.25–4.40 (m, 2H, H₁''); 7.36–7.52 (m, 3H, Ar); 7.59–7.69 (m, 4H, Ar); 8.14 (dt, $J = 8.6$; 1.9 Hz, 2H, Ar). ¹³C NMR (CDCl₃, δ): 23.0; 25.8; 28.1; 67.9; 68.5; 75.6; 127.0 (2C); 127.3 (2C); 128.1 (2C); 128.9 (2C); 130.3 (2C); 140.0; 145.7; 166.5. Chromatography in hexane/chloroform (2:8).

(±)-**Oxiran-2-ylmethyl Benzoate (23)**. Yield: 14%. $R_f = 0.32$ in chloroform. IR (CHCl₃, cm⁻¹): 1344, 1719, 2964. ¹H NMR (CDCl₃, δ): 2.74 (dd, $J = 4.9$; 2.6 Hz, 1H, 1H oxirane); 2.91 (ap t, $J = 4.5$ Hz, 1H, 1H oxirane); 3.32–3.40 (m, 1H, 1H oxirane); 4.11 (dd, $J = 12.3$; 6.2 Hz, 1H, 1H₁''); 4.60 (dd, $J = 12.3$; 3.0 Hz, 1H, 1H₁''); 7.36–7.62 (m, 3H, Ar); 8.02–8.07 (m, 2H, Ar). ¹³C

NMR (CDCl₃, δ): 43.7; 48.5; 64.4; 127.4 (2C); 128.6; 128.7 (2C); 132.2; 165.5. Chromatography in chloroform.

(±)-**Tetrahydro-2H-pyran-2-ylmethyl Benzoate (24)**. Yield: 44%. $R_f = 0.28$ hexane/chloroform (2:8). IR (CHCl₃, cm⁻¹): 1275, 1450, 1720, 2939, 3063. ¹H NMR (CDCl₃, δ): 1.33–1.62 (m, 5H, 5H tetrahydropyran); 1.81–1.84 (m, 1H, 1H tetrahydropyran); 3.34–3.47 (m, 1H, 1H tetrahydropyran); 3.57–3.67 (m, 1H, 1H tetrahydropyran); 3.93–4.00 (m, 1H, 1H tetrahydropyran); 4.21–4.30 (m, 2H, H₁''); 7.33–7.54 (m, 3H, Ar); 7.98–8.04 (m, 2H, Ar). ¹³C NMR (CDCl₃, δ): 22.9; 25.7; 28.0; 67.7; 68.3; 75.4; 128.2 (2C); 129.6 (2C); 130.1; 132.8; 166.5. Chromatography in hexane/chloroform (2:8).

(±)-**(5Z,8Z,11Z,14Z)-N-((2,2-Dimethyl-1,3-dioxolan-4-yl)methyl)icoso-5,8,11,14-tetraenamide (26)**. Yield: 43%. $R_f = 0.28$ in hexane/ethyl acetate (6:4). IR (CHCl₃, cm⁻¹): 1375, 1522, 1653, 1718, 2934. ¹H NMR (CDCl₃, δ): 0.82 (t, $J = 6.6$ Hz, 3H, H₂₀); 1.18–1.23 (m, 6H, H₁₇, H₁₈, H₁₉); 1.28 (s, 3H, CH₃); 1.36 (s, 3H, CH₃); 1.65 (qt, $J = 7.5$ Hz, 2H, H₃); 1.94–2.05 (m, 4H, H₄, H₁₆); 2.02–2.14 (m, 2H, H₂); 2.71–2.79 (m, 6H, H₇, H₁₀, H₁₃); 3.17–3.27 (m, 1H, 1H₁''); 3.45–3.49 (m, 1H, 1H₁''); 3.55 (dd, $J = 8.2$; 1.9 Hz, 1H, 1H dioxolane); 3.97 (dd, $J = 8.3$; 1.8 Hz, 1H, 1H dioxolane); 4.10–4.18 (m, 1H, 1H dioxolane); 5.22–5.40 (m, 8H, vinylic-H); 5.74 (br s, 1H, NH). ¹³C NMR (CDCl₃, δ): 13.9; 22.4; 25.0; 25.4; 25.5 (2C); 26.6; 26.7; 27.1; 29.2; 31.4; 33.8; 35.9; 41.4; 66.6; 74.6; 109.2; 122.7; 127.4; 128.0; 128.1; 128.5; 128.7; 128.9; 130.4; 172.9. Chromatography in hexane/ethyl acetate (6:4).

Data of (–)-**27** and (+)-**28** were identical to those recorded for the racemic material **1**, except for the optical rotation. (–)-**27**: $[\alpha]_D^{20} -9.1$ (c 1.5, ethanol). (+)-**28**: $[\alpha]_D^{20} +9.2$ (c 1.5, ethanol).

Data of (–)-**29** and (+)-**30** were identical to those recorded for the racemic material **4**, except for the optical rotation. (–)-**29**: $[\alpha]_D^{20} -0.7$ (c, 2 ethanol). (+)-**30**: $[\alpha]_D^{20} +0.8$ (c 2, ethanol).

Data of (–)-**31** and (+)-**32** were identical to those recorded for the racemic material **25** except for the optical rotation. (–)-**31**: $[\alpha]_D^{20} -9.4$ (c, 2 ethanol). (+)-**32**: $[\alpha]_D^{20} +10.9$ (c 2, ethanol).

Pharmacology. Enzyme Inhibition Assays. FAAH and MGL assays were undertaken using membrane and cytosolic fractions of rat cerebella.⁴² Briefly, cerebella that had been obtained previously and stored frozen were thawed and homogenized in 0.32 M sucrose containing 50 mM sodium phosphate, pH 8. Following homogenization, the samples were centrifuged at 100 000g for 60 min at 4 °C and the supernatants ("cytosolic fractions") were collected. The pellets were resuspended in 50 mM sodium phosphate, pH 8 ("membrane fractions"), and the fractions were stored frozen in aliquots until used for assay. Protein concentrations for the assays were in the range 1–3 μg/assay, the fractions being diluted with 10 mM Tris-HCl, 1 mM EDTA, pH 7.2. Each assay consisted of the fraction to be tested, test compound, substrate (³H]-2-OG or [³H]-AEA labeled in its glycerol or ethanolamine moiety respectively, final concentration 2 μM), and, when appropriate (for 2-OG-m), 3 μM URB597 in an assay volume of 200 μL. The radiolabeled substrates were obtained from American Radiolabeled Chemicals, St Louis, MO. URB597 was obtained from the Cayman Chemical Co., Ann Arbor, MI. The substrate solution contained fatty acid-free bovine serum albumin, to give an assay concentration of 0.125% w/v. After incubation for 10 min at 37 °C, reactions were stopped by the addition of 400 μL of chloroform/methanol (1:1 v/v). The tubes were capped and vortex mixed, and the phases were separated by centrifugation in a bench centrifuge. Aliquots (200 μL) of the upper phase were taken and tritium content was determined by liquid scintillation spectrometry with quench collection. Results were expressed as a % of the activity of controls containing the same volume of solvent carrier.

Acknowledgment. This work has been supported by grants from the Spanish Ministerio de Ciencia y Tecnología (SAF-2004/07103-CO2-01, SAF-2007-67008-CO2-01) and Comunidad Autónoma de Madrid (S-SAL-249-2006), the Swedish Research Council (Grant No. 12158, medicine), Konung Gustaf V's and Drottning Victorias Foundation, Gun and Bertil

Stohne's Foundation and Stiftelsen för Gamla Tjänarinnor and the Research Funds of the Medical Faculty, Umeå University. The postdoctoral research of S.V. was supported by a grant from the foundation Wenner-Grenska Samfundet. S.V. thanks the Belgian national funds for scientific research (F.N.R.S.) for the grant of postdoctoral researcher (Chargée de Recherches du F.N.R.S.). The authors thank MECT for a FPI predoctoral grant to J.A.C. J.A.C. thanks the Spanish Society of Medicinal Chemistry for the "Ramón Madroño" award.

Supporting Information Available: Table of elemental analyses of compounds 1–32. This material is available free of charge via the Internet at <http://pubs.acs.org>.

References

- Di Marzo, V.; Petrosino, S. Endocannabinoids and the regulation of their levels in health and disease. *Curr. Opin. Lipidol.* **2007**, *18*, 129–140.
- Lambert, D. M.; Fowler, C. J. The endocannabinoid system: Drug targets, lead compounds, and potential therapeutic applications. *J. Med. Chem.* **2005**, *48*, 5059–5087.
- Marsicano, G.; Lutz, B. Neuromodulatory functions of the endocannabinoid system. *J. Endocrinol. Invest.* **2006**, *29*, 27–46.
- Marsicano, G.; Wotjak, C. T.; Azad, S. C.; Bisogno, T.; Rammes, G.; Cascio, M. G.; Hermann, H.; Tang, J.; Hofmann, C.; Zieglgänsberger, W.; Di Marzo, V.; Lutz, B. The endogenous cannabinoid system controls extinction of aversive memories. *Nature* **2002**, *418*, 530–534.
- Lever, I. J.; Rice, A. S. Cannabinoids and pain. *Handb. Exp. Pharmacol.* **2007**, *177*, 265–306.
- Pagotto, U.; Marsicano, G.; Cota, D.; Lutz, B.; Pasquali, R. The emerging role of the endocannabinoid system in endocrine regulation and energy balance. *Endocr. Rev.* **2006**, *27*, 73–100.
- Centonze, D.; Finazzi-Agro, A.; Bernardi, G.; Maccarrone, M. The endocannabinoid system in targeting inflammatory neurodegenerative diseases. *Trends Pharmacol. Sci.* **2007**, *28*, 180–187.
- Karanian, D. A.; Bahr, B. A. Cannabinoid drugs and enhancement of endocannabinoid responses: Strategies for a wide array of disease states. *Curr. Mol. Med.* **2006**, *6*, 677–684.
- Ortega-Gutiérrez, S.; Molina-Holgado, E.; Arévalo-Martín, A.; Correa, F.; Viso, A.; López-Rodríguez, M. L.; Di Marzo, V.; Guaza, C. Activation of the endocannabinoid system as therapeutic approach in a murine model of multiple sclerosis. *FASEB J.* **2005**, *19*, 1338–1340.
- Bifulco, M.; Laezza, C.; Gazerro, P.; Pentimalli, F. Endocannabinoids as emerging suppressors of angiogenesis and tumor invasion. *Oncol. Rep.* **2007**, *17*, 813–816.
- Pacher, P.; Bátkai, S.; Kunos, G. The endocannabinoid system as an emerging target of pharmacotherapy. *Pharmacol. Rev.* **2006**, *58*, 389–462.
- Makara, J. K.; Mor, M.; Fegley, D.; Szabó, S. I.; Kathuria, S.; Astarita, G.; Duranti, A.; Tontini, A.; Tarzia, G.; Rivara, S.; Freund, T. F.; Piomelli, D. Selective inhibition of 2-AG hydrolysis enhances endocannabinoid signalling in hippocampus. *Nat. Neurosci.* **2005**, *8*, 1139–1141.
- Szabo, B.; Urbanski, M. J.; Bisogno, T.; Di Marzo, V.; Mendiguren, A.; Baer, W. U.; Freiman, I. Depolarization-induced retrograde synaptic inhibition in the mouse cerebellar cortex in mediated by 2-arachidonoylglycerol. *J. Physiol.* **2006**, *577*, 263–280.
- Hashimoto, Y.; Ohno-Shosaku, T.; Kano, M. Presynaptic monoacylglycerol lipase activity determines basal endocannabinoid tone and terminates retrograde endocannabinoid signaling in the hippocampus. *J. Neurosci.* **2007**, *27*, 1211–1219.
- Cravatt, B. F.; Giang, D. K.; Mayfield, S. P.; Boger, D. L.; Lerner, R. A.; Gilula, N. B. Molecular characterization of an enzyme that degrades neuromodulatory fatty-acid amides. *Nature* **1996**, *384*, 83–87.
- Cravatt, B. F.; Demarest, K.; Pacifici, M. P.; Bracey, M. H.; Giang, D. K.; Martin, B. R.; Lichtman, A. H. Supersensitivity to anandamide and enhanced endogenous cannabinoid signaling in mice lacking fatty acid amide hydrolase. *Proc. Natl. Acad. Sci. U.S.A.* **2001**, *98*, 9371–9376.
- Kathuria, S.; Gaetani, S.; Fegley, D.; Valiño, F.; Duranti, A.; Tontini, A.; Mor, M.; Tarzia, G.; La Rana, G.; Calignano, A.; Giustino, A.; Tattoli, M.; Palmery, M.; Cuomo, V.; Piomelli, D. Modulation of anxiety through blockade of anandamide hydrolysis. *Nat. Med.* **2003**, *9*, 76–81.
- Holt, S.; Comelli, F.; Costa, B.; Fowler, C. J. Inhibitors of fatty acid amide hydrolase reduce carrageenan-induced hind paw inflammation in pentobarbital-treated mice: Comparison with indomethacin and possible involvement of cannabinoid receptors. *Br. J. Pharmacol.* **2005**, *146*, 467–476.
- Jayamanne, A.; Greenwood, R.; Mitchell, V. A.; Aslan, S.; Piomelli, D.; Vaughan, C. W. Actions of the FAAH inhibitor URB597 in neuropathic and inflammatory chronic pain models. *Br. J. Pharmacol.* **2006**, *147*, 281–288.
- Goparaju, S. K.; Ueda, N.; Yamaguchi, H.; Yamamoto, S. Anandamide amidohydrolase reacting with 2-arachidonoylglycerol, another cannabinoid receptor ligand. *FEBS Lett.* **1998**, *422*, 69–73.
- de Lago, E.; Petrosino, S.; Valenti, M.; Morera, E.; Ortega-Gutiérrez, S.; Fernández-Ruiz, J.; Di Marzo, V. Effect of repeated systemic administration of selective inhibitors of endocannabinoid inactivation on rat brain endocannabinoid levels. *Biochem. Pharmacol.* **2005**, *70*, 446–452.
- Jhaveri, M. D.; Richardson, D.; Kendall, D. A.; Barrett, D. A.; Chapman, V. Analgesic effects of fatty acid amide hydrolase inhibition in a rat model of neuropathic pain. *J. Neurosci.* **2006**, *26*, 13318–13327.
- Maione, S.; Bisogno, T.; de Novellis, V.; Palazzo, E.; Cristino, L.; Valenti, M.; Petrosino, S.; Guglielmotti, V.; Rossi, F.; Di Marzo, V. Elevation of endocannabinoid levels in the ventrolateral periaqueductal grey through inhibition of fatty acid amide hydrolase affects descending nociceptive pathways via both cannabinoid receptor type 1 and transient receptor potential vanilloid type-1 receptors. *J. Pharmacol. Exp. Ther.* **2006**, *316*, 969–982.
- Lichtman, A. H.; Hawkins, E. G.; Griffin, G.; Cravatt, B. F. Pharmacological activity of fatty acid amides is regulated, but not mediated, by fatty acid amide hydrolase in vivo. *J. Pharmacol. Exp. Ther.* **2002**, *302*, 73–79.
- Sugiura, T.; Kishimoto, S.; Oka, S.; Gokoh, M. Biochemistry, pharmacology and physiology of 2-arachidonoylglycerol, an endogenous cannabinoid receptor ligand. *Prog. Lipid Res.* **2006**, *45*, 405–446.
- Dinh, T. P.; Carpenter, D.; Leslie, F. M.; Freund, T. F.; Katona, I.; Sensi, S. L.; Kathuria, S.; Piomelli, D. Brain monoglyceride lipase participating in endocannabinoid inactivation. *Proc. Natl. Acad. Sci. U.S.A.* **2002**, *99*, 10819–10824.
- Karlsson, M.; Contreras, J. A.; Hellman, U.; Tornqvist, H.; Holm, C. cDNA cloning, tissue distribution, and identification of the catalytic triad of monoglyceride lipase. *J. Biol. Chem.* **1997**, *272*, 27218–27223.
- Viso, A.; Cisneros, J. A.; Ortega-Gutiérrez, S. The medicinal chemistry of agents targeting monoacylglycerol lipase. *Curr. Top. Med. Chem.* **2007**, in press.
- Cravatt, B. F.; Saghatelian, A.; Hawkins, E. G.; Clement, A. B.; Bracey, M. H.; Lichtman, A. H. Functional dissociation of the central and peripheral fatty acid amide signalling systems. *Proc. Natl. Acad. Sci. U.S.A.* **2004**, *101*, 10821–10826.
- Bracey, M. H.; Hanson, M. A.; Masuda, K. R.; Stevens, R. C.; Cravatt, B. F. Structural adaptations in a membrane enzyme that terminates endocannabinoid signaling. *Science* **2002**, *298*, 1793–1796.
- Boger, D. L.; Miyauchi, H.; Du, W.; Hardouin, C.; Fecik, R. A.; Cheng, H.; Hwang, I.; Hedrick, M. P.; Leung, D.; Acevedo, O.; Guimaraes, C. R. W.; Jorgensen, W. L.; Cravatt, B. F. Discovery of a potent, selective, and efficacious class of reversible α -keto-heterocycle inhibitors of fatty acid amide hydrolase effective as analgesics. *J. Med. Chem.* **2005**, *48*, 1849–1856.
- Alexander, J. P.; Cravatt, B. F. Mechanism of carbamate inactivation of FAAH: implications for the design of covalent inhibitors and in vivo functional probes for enzymes. *Chem. Biol.* **2005**, *12*, 1179–1187.
- Romero, F. A.; Du, W.; Hwang, I.; Rayl, T. J.; Kimball, F. S.; Leung, D.; Hoover, H. S.; Apodaca, R. L.; Breitenbucher, J. G.; Cravatt, B. F.; Boger, D. L. Potent and selective α -keto-heterocycle-based inhibitors of the anandamide and oleamide catabolizing enzyme, fatty acid amide hydrolase. *J. Med. Chem.* **2007**, *50*, 1058–1068.
- Saario, S. M.; Salo, O. M. H.; Nevalainen, T.; Poso, A.; Laitinen, J. T.; Järvinen, T.; Niemi, R. Characterization of the sulfhydryl-sensitive site in the enzyme responsible for hydrolysis of 2-arachidonoylglycerol in rat cerebellar membranes. *Chem. Biol.* **2005**, *12*, 649–656.
- Bisogno, T.; Howell, F.; Williams, G.; Minassi, A.; Cascio, M. G.; Ligresti, A.; Matias, I.; Schiano-Moriello, A.; Paul, P.; Williams, E. J.; Gangadharan, U.; Hobbs, C.; Di Marzo, V.; Doherty, P. Cloning of the first sn-1-DAG lipases points to the spatial and temporal regulation of endocannabinoid signaling in the brain. *J. Cell. Biol.* **2003**, *163*, 463–468.

- (36) Dinh, T. P.; Kathuria, S.; Piomelli, D. RNA interference suggests a primary role for monoacylglycerol lipase in the degradation of the endocannabinoid 2-arachidonoylglycerol. *Mol. Pharmacol.* **2004**, *66*, 1260–1264.
- (37) Goparaju, S. K.; Ueda, N.; Taniguchi, K.; Yamamoto, S. Enzymes of porcine brain hydrolyzing 2-arachidonoylglycerol, an endogenous ligand of cannabinoid receptors. *Biochem. Pharmacol.* **1999**, *57*, 417–423.
- (38) Muccioli, G. G.; Xu, C.; Odah, E.; Cudaback, E.; Cisneros, J. A.; Lambert, D. M.; López-Rodríguez, M. L.; Bajjalieh, S.; Stella, N. Identification of a novel endocannabinoid-hydrolyzing enzyme expressed by microglial cells. *J. Neurosci.* **2007**, *27*, 2883–2889.
- (39) Hohmann, A. G.; Suplita, R. L.; Bolton, N. M.; Neely, M. H.; Fegley, D.; Mangieri, R.; Krey, J. F.; Walker, J. M.; Holmes, P. V.; Crystal, J. D.; Duranti, A.; Tontini, A.; Mor, M.; Tarzia, G.; Piomelli, D. An endocannabinoid mechanism for stress-induced analgesia. *Nature* **2005**, *435*, 1108–1112.
- (40) Holt, S.; Paylor, B.; Boldrup, L.; Alajakku, K.; Vandevorde, S.; Sundström, A.; Cocco, M. T.; Onnis, V.; Fowler, C. J. Inhibition of fatty acid amide hydrolase, a key endocannabinoid metabolizing enzyme, by analogues of ibuprofen and indomethacin. *Eur. J. Pharmacol.* **2007**, *565*, 26–36.
- (41) Ghafouri, N.; Tiger, G.; Razdan, R. K.; Mahadevan, A.; Pertwee, R. G.; Martin, B. R.; Fowler, C. J. Inhibition of monoacylglycerol lipase and fatty acid amide hydrolase by analogues of 2-arachidonoylglycerol. *Br. J. Pharmacol.* **2004**, *143*, 774–784.
- (42) Vandevorde, S.; Saha, B.; Mahadevan, A.; Razdan, R. K.; Pertwee, R. G.; Martin, B. R.; Fowler, C. J. Influence of the degree of unsaturation of the acyl side chain upon the interaction of analogues of 1-arachidonoylglycerol with monoacylglycerol lipase and fatty acid amide hydrolase. *Biochem. Biophys. Res. Commun.* **2005**, *337*, 104–109.
- (43) Fowler, C. J.; Tiger, G. Cyclooxygenation of the arachidonoyl side chain of 1-arachidonoylglycerol and related compounds block their ability to prevent anandamide and 2-oleoylglycerol metabolism by rat brain in vitro. *Biochem. Pharmacol.* **2005**, *69*, 1241–1245.
- (44) Saario, S. M.; Savinainen, J. R.; Laitinen, J. T.; Järvinen, T.; Niemi, R. Monoglyceride lipase-like enzymatic activity is responsible for hydrolysis of 2-arachidonoylglycerol in rat cerebellar membranes. *Biochem. Pharmacol.* **2004**, *67*, 1381–1387.
- (45) Vandevorde, S.; Jonsson, K.-O.; Labar, G.; Persson, E.; Lambert, D. M.; Fowler, C. J. Lack of selectivity of URB602 for 2-oleoylglycerol compared to anandamide hydrolysis in vitro. *Br. J. Pharmacol.* **2007**, *150*, 186–191.
- (46) Makara, J. K.; Mor, M.; Fegley, D.; Szabó, S. I.; Kathuria, S.; Astarita, G.; Duranti, A.; Tontini, A.; Tarzia, G.; Rivara, S.; Freund, T. T.; Piomelli, D. Corrigendum: Selective inhibition of 2-AG hydrolysis enhances endocannabinoid signalling in hippocampus. *Nat. Neurosci.* **2007**, *10*, 134.
- (47) Saario, S. M.; Palomäki, V.; Lehtonen, M.; Nevalainen, T.; Järvinen, T.; Laitinen, J. T. URB754 has no effect on the hydrolysis or signaling capacity of 2-AG in the rat brain. *Chem. Biol.* **2006**, *13*, 811–814.
- (48) Jonsson, K.-O.; Vandevorde, S.; Lambert, D. M.; Tiger, G.; Fowler, C. J. Effects of homologues and analogues of palmitoylethanolamide upon the inactivation of the endocannabinoid anandamide. *Br. J. Pharmacol.* **2001**, *133*, 1263–1275.
- (49) Thors, L.; Fowler, C. J. Is there a temperature-dependent uptake of anandamide into cells? *Br. J. Pharmacol.* **2006**, *149*, 73–81.
- (50) Vandevorde, S.; Jonsson, K.-O.; Fowler, C. J.; Lambert, D. M. Modifications of the ethanolamine head in *N*-palmitoylethanolamine: synthesis and evaluation of new agents interfering with the metabolism of anandamide. *J. Med. Chem.* **2003**, *46*, 1440–1448.
- (51) Boldrup, L.; Wilson, S. J.; Barbier, A. J.; Fowler, C. J. A simple stopped assay for fatty acid amide hydrolase avoiding the use of a chloroform extraction phase. *J. Biochem. Biophys. Methods* **2004**, *60*, 171–177.
- (52) Bisogno, T.; Cascio, M. G.; Saha, B.; Mahadevan, A.; Urbani, P.; Minassi, A.; Appendino, G.; Saturnino, C.; Martin, B.; Razdan, R.; Di Marzo, V. Development of the first potent and specific inhibitors of endocannabinoid biosynthesis. *Biochim. Biophys. Acta* **2006**, *1761*, 205–212.
- (53) López-Rodríguez, M. L.; Viso, A.; Ortega-Gutiérrez, S.; Fowler, C. J.; Tiger, G.; de Lago, E.; Fernández-Ruiz, J.; Ramos, J. A. Design, synthesis and biological evaluation of new inhibitors of the endocannabinoid uptake: comparison with effects on fatty acid amidohydrolase. *J. Med. Chem.* **2003**, *46*, 1512–1522.

JM070642Y